Analysis of the Droplet Ejection for Piezoelectric-driven Industrial Inkjet Head

Wonchul Sim, Sung-Jun Park, Changsung Park, Youngseuck Yoo,
Youngjae Kim, Jaewoo Joung and Yongsoo Oh

eMD Lab., Central R&D Institute, Samsung Electro-Mechanics Co. Ltd.,
#314 Meatan 3 dong, Suwon, Gyeonggi-do, Korea, wc.sim@samsung.com

ABSTRACT

A hybrid design tool combining one-dimensional (1D) lumped parameter model and three-dimensional (3D) computational fluid dynamics (CFD) approach has been developed and applied to industrial inkjet head design for the application of direct writing on printed circuit boards (PCB). Lumped element modeling technique is applied to simplify the composite Inkjet print head system and the calculation of lumped parameters such as compliance, resistance and inertance is explained theoretically. Performance of 1D analysis shows that it is useful for the evaluation of a proposed design of inkjet head.

Time sequence of droplet generation is verified by the comparison between 3D analysis result and photographic images acquired by stroboscopic technique. The developed model helps to understand the drop formation process and influence of flow part on the jetting performance.

Keywords: 1D lumped element model, CFD, inkjet printing head, drop formation

1 INTRODUCTION

Recently, inkjet printing method has been investigated in order to replace the conventional high-cost micro patterning processes on the electronic products which include the repetition of mask masking, UV exposure, developing, chemical etching, resist stripping, cleaning, water rinsing and drying[1]. With the recent advances in synthesis and stabilization of nano-particle in specific medium[2], inkjet printing become a promising solution of the distribution and patterning of materials for a wide variety of application[3,4]. Compared with the conventional process, inkjet printing technology has the benefits of low cost, simpler processing, and a high rate of material utilization.

To eject a fine droplet, several kinds of actuation method has been studied. The thermal and piezoelectric actuation methods are commercially successful technologies. However, thermal actuation could damage to the property of conductive nano-particles dispersed in the ink. Hence, the adoption of the reliable piezoelectric inkjet printing technology considered to be desired for the inkjet printing. However, absence of the reliable piezoelectric inkjet head for various functional inks prevents the application on the manufacturing electronic products due to precise control of droplet size and elimination of the satellite droplet[5~7].

In this study, we investigate the bending mode piezoelectric inkjet head for the application of metal liquid printing on PCBs. In order to predict the performance of the inkjet head, lumped element model is developed. Also, we present the development of the computer aided engineering(CAE) tools for inkjet head design optimization and verification of the head performance of industrial inkjet heads to provide novel design concepts of metal jetting head for printing on PCBs.

2 1D LUMPED MODEL

Schematic view of the piezoelectric-driven drop-on-demand inkjet head is shown in Fig. 1. Inkjet printing head includes a reservoir which contains ink, a restrictor, a pressurization chamber which receives the ink from the reservoir through the restrictor, a nozzle having orifice which receive ink from the pressurization chamber and a piezoelectric transducer. The pressurization chamber has a vibratory plate which forms a portion of a wall of the pressurization chamber and a piezoelectric element couple to the vibratory plate. When an electric field is applied to a piezoelectric material, it changes its planar dimensions. However, it is rigidly attached to the vibratory plate, bending occurs. This bending increases the pressure in a chamber and causes the ink droplet to be ejected through the nozzle.

As mentioned above, the demand type ink jet head are composed of a composite system of electrical, mechanical, and fluidic elements. In order to simplify the complex system, lumped element modeling technique can be adapted for describing inkjet system. On the other hand, the mathematical difficulty of predicting the performance of the printing head is greatly reduced by replacing the distributed components with equivalent lumped elements[8,9].

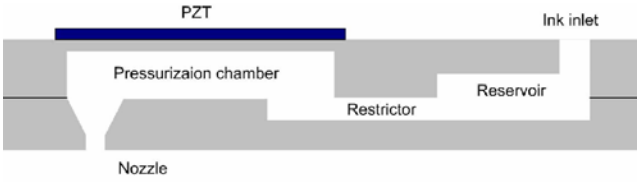

Figure 1: Structure of piezoelectric inkjet head.

The displacement of a piezoelectric vibrator on a pressurization chamber, and the resulting ink stream, may be analogized to an electric circuit as shown in Fig. 2. C, M, and R illustrate the compliance, inertance and resistance of the lumped elements respectively. Fluid compressibility in pressurization chamber is represented by C, compliance. Also, elastic deformation of vibratory plate acts as compliance. When accelerated ink flows through a thin passage, the mass of the ink acts as inertance. Under this analysis, the ink jet printing head is like a series circuit as shown in Fig. 2. In the notation, the subscript denotes the component in the inkjet head.(e.g., "p" for piezoelectric vibrator, "c" for pressure generating chamber, "r" for restrictor, "n" for nozzle, "res" for reservoir and "m" for meniscus.) By using lumped element modeling of inkjet printing head, derived Eq.(1) and (2) are as follows:

$$\ddot{q}_r = -\frac{1}{M_r}\left\{R_r \dot{q}_r + \frac{1}{C_p + C_c} q_r + \frac{1}{C_p + C_c} q_n - \frac{C_p}{C_p + C_c} V_p + V_{res}\right\} \quad (1)$$

$$\ddot{q}_n = -\frac{1}{M_n}\left\{R_n \dot{q}_n + \frac{1}{C_p + C_c} q_r + \frac{1}{C_p + C_c} q_n - \frac{C_p}{C_p + C_c} V_p + V_m\right\} \quad (2)$$

where $\ddot{q}_r$ and $\ddot{q}_n$ are flow rate in restrictor and nozzle, respectively. Fig. 3 shows the block diagram of equivalent circuit for inkjet printing head. Compared with inertance and resistance of nozzle and restrictor, M_c and R_c are relatively small that they can be neglected.

2.1 Piezoelectric vibrator

An AC voltage V_p is applied across the piezoelectric vibrator to generate an effective pressure that drives diaphragm into oscillation. Thus, a conversion ratio [K_{VtoP}] from electrical domain to fluidic with units of [Pa/V] should be considered [4]. The K_{VtoP} can be calculated by comparison between the displacement generated by applied voltage and by pressure. In order to obtain compliance of piezoelectric vibrator and K_{VtoP}, finite element(FE) analysis has been performed using commercial FEM package CoventorWare™. As shown in Fig. 4, the three dimensional FE model has been created and voltage and pressure are applied to the composite plate. It shows the simulated

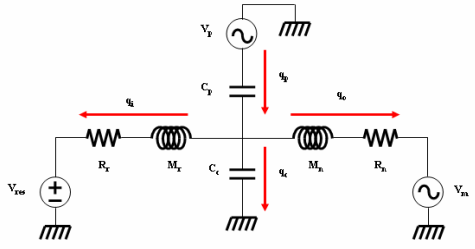

Figure 2: Equivalent circuit representation of a piezo – driven inkjet system.

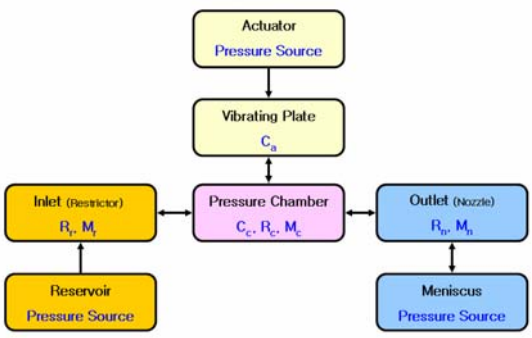

Figure 3: Block diagram of 1D lumped model for inkjet head.

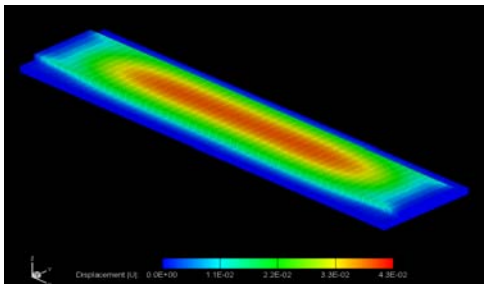

Figure 4: Simulated displacement corresponding to an applied voltage for calculation of the compliance of vibrator and K_{VtoP} for lumped element analysis.

displacement contour of piezoelectric vibrator to acquire the compliance of piezoelectric vibrator and conversion ratio of voltage to pressure which are described as follows:

$$C_p = \frac{V_a}{P} \quad (3)$$

$$K_{VtoP} = \frac{\left(\frac{V_v}{C_p}\right)}{v} \quad (4)$$

where V_a is a volume change by pressure, P is an applied pressure, V_v is a volume change by voltage, and v is an applied voltage.

2.2 Flow part

Fluid compressibility of pressurization chamber acts as compliance. The compliance of pressurization chamber is given by

$$C_c = \frac{V_c}{\rho \alpha^2} \quad (5)$$

where V_c is the volume of the pressurization chamber, ρ is the density of ink and α is the speed of sound in ink which is about 1500 m/s.

Pressure drop is caused by viscous losses in the channels of the inkjet. In addition, when fluid moves through the flow passages, the sudden change of cross-sectional area occurs between both restrictor and nozzle and pressurization chamber as shown in Fig. 5. Thus, the sudden expansion and contraction of cross-sectional area should be considered for the calculation of pressure drop.

$$\Delta P = R\dot{q} + R_{se}\dot{q}^2 + R_{sc}\dot{q}^2 \tag{6}$$

where $\dot{q}$ is flow rate and R_{se} and R_{sc} are the resistance at sudden expansion and contraction. Based on Eq. (6) fallowing equations are given by

$$\Delta P_{res} = R_r\dot{q}_i + R_{se}\dot{q}_i^2 + R_{sc}\dot{q}_i^2 \tag{7}$$

$$\Delta P_{nol\_in} = R_n\dot{q}_o + R_{se}\dot{q}_o^2 \tag{8}$$

$$\Delta P_{nol\_out} = R_n\dot{q}_o + R_{sc}\dot{q}_o^2 \tag{9}$$

where R_r and R_n is fallows as:

$$R_r = 128\mu\frac{L_r}{\pi\cdot D_{eff\_r}^2} \tag{10}$$

$$R_n = 128\mu\frac{L_r}{\pi\cdot D_n^2} \tag{11}$$

where L_r is length of restrictor, L_n is the length of nozzle, μ is the ink viscosity, D_{eff_r} is the effective diameter of restrictor, and D_n is the diameter of nozzle. The resistance due to change of cross-section is given by

$$R_{se} = \frac{\rho k_{se}}{2\times A^2} \tag{12}$$

$$R_{sc} = \frac{\rho k_{sc}}{2\times A^2} \tag{13}$$

where A is the cross-sectional area of sudden expansion and contraction, K_{se} is the loss coefficient of sudden expansion and K_{sc} is the loss coefficient of sudden contraction which are empirically determined.

The pressure generated by deflecting an elastic vibrator keeps the balance with the action of surface tension of the fluid in the orifice. In order to estimate the pressure of the meniscus with a circular cross section as shown in Fig.6,

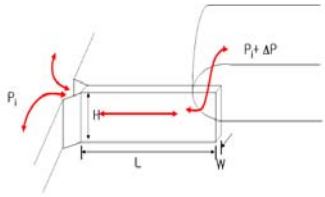

(a)Flow from restrictor to chamber and vice versa

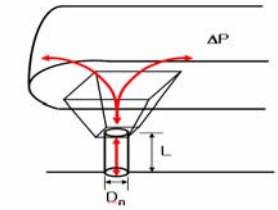

(b)Flow from nozzle to chamber and vice versa

Figure 5: The flow in restrictor and nozzle parts.

we assume that the profile of meniscus maintains a parabolic shape as presented in Eq. (14).

$$z = Z_{\max}\left(1-\frac{r^2}{R^2}\right) \tag{14}$$

The meniscus pressure driven by equilibrium condition with surface tension is as fallows:

$$\Delta P = \frac{4\sigma}{D_n}\sqrt{\frac{16\cdot Z_{\max}^2}{16\cdot Z_{\max}^2 + D_n^2}} \tag{15}$$

where Z_{max} is the maximum displacement of meniscus, R is radius of nozzle and σ is surface tension.

When ink flows through a thin passage, the inertia of the ink is represented by inertance. The inertance is given by

$$M = \beta\cdot\rho\frac{L}{A} \tag{16}$$

where β is a empirical coefficient and A is the cross-section area.

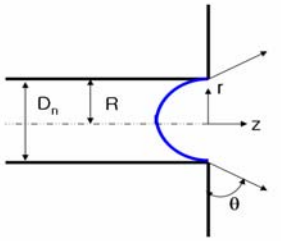

Figure 6: The meniscus with circular orifice.

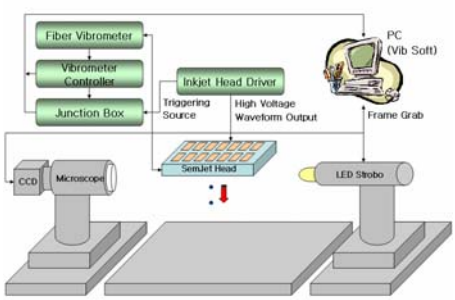

Figure 7: The schematic diagram of overall visualization equipment.

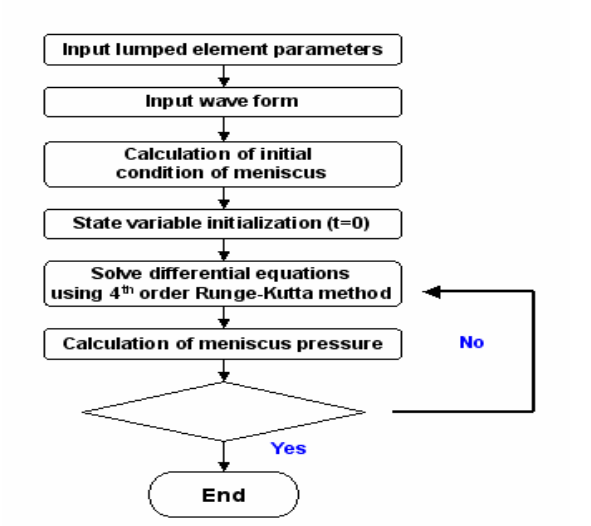

Figure 8: Flow chart of 1D program.

3 RESULT AND DISSCUSION

To investigate the performance of the printing head with respect to drop velocity and drop diameter the stroboscopic visualization technique was used. The stroboscope system (Fig. 7) consists of a high-resolution CCD camera, LDV system, a stroboscope, and a PC with driving waveform control unit.

3.1 Lumped elements of inkjet system

For an inkjet printing head, the value of compliance and inertance are obtained by using Eq. (3),(5) and (16) and tabulated in Table 1. The K_{VtoP} acquired by Eq. (4) is 2.36 x 10^4 Pa/V. The resistance of the restrictor and nozzle are calculated by Eq. (10) and (11) for the given geometry. The resistance at sudden expansion occurs when flow moves from restrictor to both reservoir and pressurization chamber. The resistance of nozzle at sudden expansion appears as it passes from nozzle to chamber. On the contrary, the resistance at sudden contraction vice versa. The calculated resistances are listed in Table 2.

3.2 1D analysis

1D lumped model solutions are numerically obtained by using a fourth-order Runge-Kutta integration algorithm to solve the differential equations using MATLAB. Flow chart of the program is shown in Fig. 8. After preparation of lumped element parameters for calculation, the analysis is completed within one minute. Therefore, the time efficiency of 1D analysis is quite competitive compared with time consuming 3D analysis.

When the voltage waveform with a rectangular shape as shown in Fig.9 is applied to the piezoelectric vibrator, the droplet velocity and ejection volume has been observed. The waveform consists of three parts of rising time(T_r), pulse width(T_h) and falling time(T_f). The driving voltage is 30V and T_r, T_h and T_f are 2 μs, 3 μs and 5 μs, respectively. In this work, viscosity and surface tension of ink is 4.8 cPs and 0.025 N/m, respectively. Comparison between simulation result and measured one is shown in Table 2. Both the predicted droplet velocity and the drop volume match well with the experimental results. By using 1D analysis, the characteristics of droplet velocity and ejected volume with time variation are shown in Fig. 9.

Some difference between the measured data and the theoretical one results from inaccurate resistance. The theoretical equation used for calculation is not implemented for obtaining the exact value of resistance of flow passage. Alternatively, 3D modeling approach can be used for improving accuracy of lumped model.

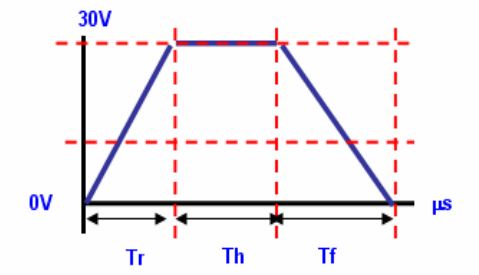

Figure 9: Waveforms of the driving voltages signal applied to the inkjet head.

		Unit	Value
Compliance	C_p	m^5/N	2.0 x 10^{-19}
	C_c		2.0 x 10^{-19}
Inertance	M_r	kg/m^2	4.25 x 10^8
	M_n		5.86 x 10^8

Table 1: The calculated compliance and inertance

		Unit	Value
R_n		Ns/m^5	1.61×10^{13}
R_r			7.24×10^{12}
Restrictor to reservoir	$R_{r,se}$	Ns^2/m^8	3.15×10^{19}
Chamber to restrictor	$R_{r,sc}$		1.36×10^{19}
Chamber to nozzle	$R_{n,sc}$		4.19×10^{20}
Restrictor to chamber	$R_{r,se}$		1.92×10^{19}
Reservoir to restrictor	$R_{r,sc}$		1.06×10^{19}
Nozzle to chamber	$R_{n,se}$		9.91×10^{20}

Table 2: Resistances for 1D lumped model analysis

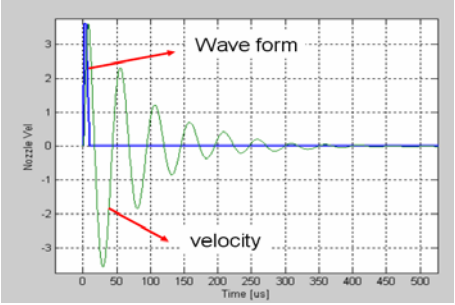

(a) Droplet velocity vs. time

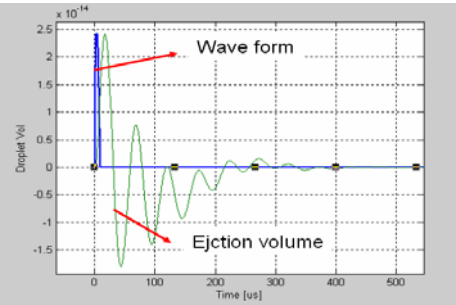

(b) Ejection volume vs. time

Figure 9: Results of 1D lumped model.

	1D analysis	Measurement	Error(%)
Droplet volume[pl]	24.2	27.5	12
Droplet velocity[m/s]	3.6	3.8	6

Table 2: Comparison between simulation result and measurement.

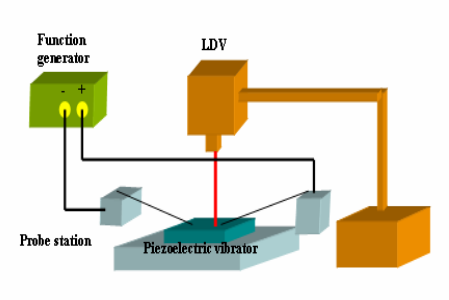

(a) LDV experimental set-up

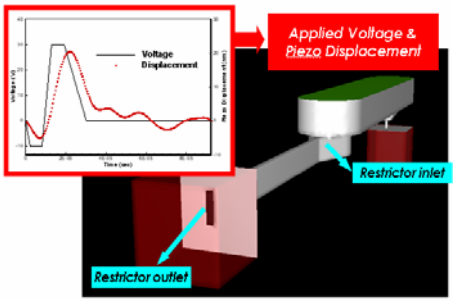

(b) Measured displacement curve

Figure 10: The input displacement data for 3D droplet formation analysis.

3.3 Droplet formation analysis

To explore the liquid ejection behavior which can not be performed by 1D analysis, three-dimensional computation model for inkjet model is studied with a commercial computational fluid dynamics solver of CFD-ACE. To reduce the error between measured data and simulated one, an accurate input data should be provided. Therefore, the bending deflection of the piezoelectric vibrator according to the applied driving waveform is measured by means of a Laser Doppler Vibrometer (LDV) at the top of the pressurization chamber. Fig. 10 shows the schematic diagram of the LDV experimental set-up and obtained displacement curve for the input of simulation.

The visual observation of an ejected droplet at the real printing head is compared with the graphic evaluation of the simulation results as shown in Fig. 11. As can be seen in the figure, a comparison between the simulation results and the photographical images of the ejected droplets shows good agreement with time sequence.

4 CONCLUSION

In this paper, the modeling approach combining 1D analysis and 3D analysis has been developed and applied to industrial inkjet head design. The inkjet printing system is simplified to the equivalent electric circuit and lumped elements are acquired by theoretically driven equations.

1D analysis has advantage of evaluating the performance of the designed inkjet printing head in a short

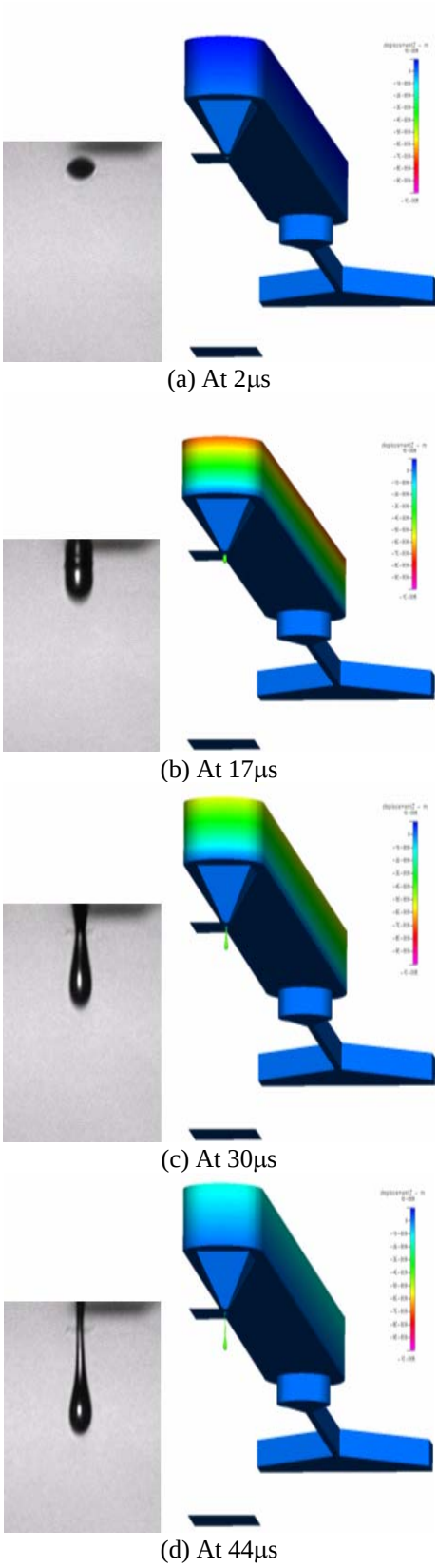

(a) At 2μs

(b) At 17μs

(c) At 30μs

(d) At 44μs

Figure 11: Comparison between the measured and simulated drop formations with time interval.

time. And, the droplet formation process achieved by 3D analysis is expected to help to understand the effect on the driving voltage waveform for the increase of droplet velocity and reduction of droplet size for the application of the direct writing on printed circuit boards(PCB).

Our modeling approach as presented here can be used as a design tool for a better design of piezoelectric inkjet printing head to improve the jetting performance

REFERENCES

[1] Ryoichi Ohigashi and Katsunori Tsuchiya, "Micro Capillaries Array Head for Direct Drawing of Fine Patterns'', IEEE MEMS 2001, pp. 389-392.

[2] K. L. Lelly, T. R. Jensen, A. A. Lazarides, G. C. Schatz, in: "Metal Nanoparticles: Synthesis, Charaterization and Applications", D.L. Feldheim, C. A. Foss, Eds., Marcel Dekker, New York 2002, Chapter 4, pp. 89-118.

[3] P. E. J. Legierse, "Inkjet Printing in the Electronics Industry", DDP2001, pp. 197-200.

[4] Stephen F. Pond, "Inkjet Technology and Product Development Strategies", Torrey Pines Research, Carlsbad, 2000.

[5] Donald J. Hayes et al., "Printing System for MEMS Packaging ", SPIE Conference on Micromachining and Microfabrication, pp. 1-9, October, 2001

[6] David Wallace et al., 'Think additive: Ink-jet Deposition of Materials for MEMS Packaging", 6th Topical Workshop on Packaging of MEMS and Related Micro-Nano-Bio integrated Systems, pp 1-5, November 18-20, 2004

[7] Tanya Kaydanova et al., "Ink Jet Printing Approaches to Solar Cell Contacts", NCPV and Solar Program Review Meeting, pp. 919-920, 2003

[8] E. L. Kyser, L. F.Collins and N. Herbert, "Design of an Impulse Ink Jet", Journal of Applied Photographic Engineering. Vol. 7, 1981, pp.73-79

[9] E. L. Kyser and S. B. Sears, "Method and apparatus for recording with writing fluids and drop projection means therefore", U.S. Patent no. 3,946,398, Siliconics Inc., 1976.